Journal of Drug Delivery Science and Technology 55 (2020) 101472

Contents lists available at ScienceDirect

Journal of Drug Delivery Science and Technology

journal homepage: www.elsevier.com/locate/jddst

Miscibility and sustained release of drug from cellulose acetate butyrate/caffeine films

Laíse M. Furtado[a], Karina C.P. Hilamatu[a], Krishnasamy Balaji[b], Rômulo A. Ando[a], Denise F.S. Petri[a,*]

[a] Department of Fundamental Chemistry, Institute of Chemistry - University of São Paulo, Av. Prof. Lineu Prestes 748, São Paulo, 05508-000, Brazil
[b] Polymer Engineering Laboratory, PSG Institute of Technology and Applied Research, Neelambur, Coimbatore, 641062, India

ARTICLE INFO

Keywords:
Caffeine
Cellulose acetate butyrate
Drug release
Miscibility
FTIR-ATR
DFT calculation

ABSTRACT

The miscibility of caffeine and cellulose acetate butyrate (CAB) was investigated as a function of caffeine (caf) content and correlated with *in vitro* drug release studies. Films of CAB/caf with caffeine contents larger than 5 wt % presented partial miscibility, as revealed by scanning electron microscopy, turbidity measurements and thermogravimetric analyses. CAB/caf with 2.5 wt% or less were homogeneous films. Favorable interactions between CAB and caffeine was evidenced by the decrease of the glass transition temperature of CAB in 28 °C and by Fourier transform infrared vibrational spectra of the films, which displayed shifts to higher wavenumbers of caffeine bands assigned to the stretching of conjugated C=O(6) and isolated C=O(2) carbonyl groups of 16 cm^{-1} and 9 cm^{-1}, respectively. No drug was released from completely miscible systems, regardless of the external medium. Partially miscible CAB/caf systems showed a two-step release process: in the first 6 h the segregated portion of caffeine dissolved in the medium and a second one, when the release of drug located in the internal polymer matrix took place. After 48 h, at pH 7.4, the release of caffeine from CAB/caf 7 wt% was complete.

1. Introduction

The esterification of cellulose enables a range of properties that are impossible for raw cellulose; one of them is the possibility of extrusion, injection, and dissolution in common organic solvents. Such properties make cellulose esters useful for the development of coatings, paint, and sensors [1]. Cellulose acetate butyrate (CAB) has been an important component for coating formulations because it reduces dry time, improves flow and leveling, and controls viscosity [1]. CAB biocompatibility allows its application as drug release system [2–6] and as efficient support for enzymes [7] and lectins [8].

Caffeine or 1,3,7-trimethylxanthine is an alkaloid belonging to the purine family, which exerts various stimulating effects on the central nervous system and can act as immunomodulatory [9]. There is significant interest for caffeine carriers that allow its sustained release, because caffeine absorption is very rapid and reaches 99% absorption after 45 min ingestion [10]. Among many reported carriers, polysaccharides have been often used to encapsulate caffeine due to their ability to swell, biocompatibility and nontoxicity [11–16]. Cellulose and cellulose esters also present such advantageous properties and allow designing different architectures, such as macroporous beads [17] and core-shell nanofibers [18]. Microfibrillated cellulose coated paper served as an interesting carrier for caffeine, which was completely released after 10 h [19]. CAB combined with Eudragit®, a hydrophilic acrylate based copolymer, and triacetate citrate, a plasticizer, resulted in mechanically stable membrane to coat osmotic tablets for caffeine release [6]. Cellulose esters have been used as coating for osmotic tablets; the tablet is coated with a semi-permeable membrane (cellulose ester) and a laser drills holes in it. Upon contacting gastrointestinal fluids, the membrane swells by osmosis, dissolving the drug and pushing it towards the gastrointestinal tract [20].

Despite the interesting reports available in the literature, a systematic study about the miscibility of caffeine and CAB and its influence on the sustained release of caffeine is still missing. In this study, the miscibility of caffeine and CAB was systematically investigated as nanometric spin-coated and micrometric cast CAB/caffeine films with different caffeine contents by means of morphological and structural analyses, turbidity and differential scanning calorimetry (DSC). DSC gives information about the glass transition temperature (T_g) of polymer chains; in the presence of second component, the mobility of

* Corresponding author.
E-mail addresses: laise_furtado@usp.br (L.M. Furtado), karinahilamatu@hotmail.com (K.C.P. Hilamatu), balaji.psgtech@yahoo.co.in (K. Balaji), raando@iq.usp.br (R.A. Ando), dfsp@iq.usp.br (D.F.S. Petri).

https://doi.org/10.1016/j.jddst.2019.101472
Received 26 October 2019; Received in revised form 29 November 2019; Accepted 18 December 2019
Available online 23 December 2019
1773-2247/

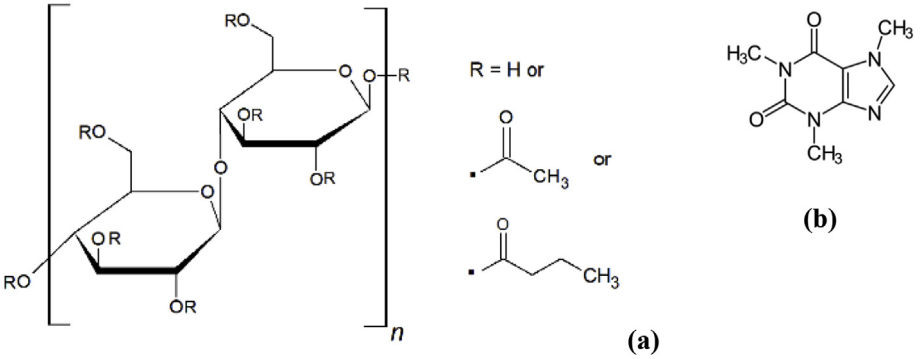

Fig. 1. Schematic representation of chemical structures of (a) CAB repeating units and (b) caffeine.

polymer chains might increase due to favorable interactions, decreasing the T_g value. Therefore, if CAB and caffeine are miscible, the T_g value of CAB is expected to decrease. The *in vitro* release behavior of caffeine from CAB/caffeine films under different pH and ionic strength was investigated and correlated with the miscibility of caffeine and CAB.

2. Material and methods

2.1. Materials

Cellulose acetate butyrate (CAB, Eastman, DS_{Ac} = 0.2, DS_{But} = 2.5, M_v ~ 30,000 g mol^{-1}, USA), caffeine (caf, Sigma W222402, 194.19 g mol^{-1}, purity 99.9%) toluene (LabSynth, Brazil), ethyl acetate (EA, LabSynth, Brazil) and acetone (Ace, LabSynth, Brazil) were used as received. The chemical structures of CAB and caf are represented in Fig. 1.

2.2. Preparation of thin films by spin-coating and characterization

CAB was dissolved in ethyl acetate (EA) at 10 g L^{-1}, 20 g L^{-1} and 40 g L^{-1}. CAB solution was mixed with caffeine (caf) dissolved in acetone at 10 g L^{-1}, at the volume ratio 1:1, so that the final concentrations were reduced to one-half their original values. The samples were coded as CAB5/caf, CAB10/caf, CAB20/caf. The initial concentration of caffeine was chosen at 10 g L^{-1} to ensure complete dissolution.

Thin films were prepared by spin-coating on Si/SiO_2 wafers and glass slides, with a Headway PWM32-PS-R790 spinner operating at 3000 rpm for 30 s, at (24 ± 1) °C and (75 ± 5)% of relative humidity. The thickness of the films was determined by ellipsometry in a vertical computer-controlled DRE-EL02 ellipsometer; the angle of incidence was set at 70.0° and the wavelength of the He–Ne laser was 632.8 nm [7,8]. The morphology of spin-coated films on Si/SiO_2 wafers was analyzed by scanning electron microscopy (SEM) in a SEM-FEG JEOL JSM7401F microscope; the surfaces were coated with a 2 nm thick gold layer prior to the analyses. Spin-coated films glass slides were characterized by confocal fluorescence microscopy (CFM) in a Zeiss LSM 510 equipment, the $\lambda_{excitation}$ and $\lambda_{emission}$ for caffeine were 559 nm and 637 nm, respectively.

2.3. Preparation of micrometric films by casting and characterization

Micrometric films were prepared by casting CAB/caf solution on Petri dishes and heating at 60 °C until complete solvent evaporation. The thickness of the films was measured with a Mitutoyo Thickness Gage (Type ID-C1012XBS; Mitutoyo Manufacturing Co. Ltd, Kawasaki, Japan), being measured at three randomly chosen different positions of at least two films of same composition. Solutions of CAB in EA (20 g L^{-1}) were mixed with caffeine solution in acetone at different concentrations, so that after drying the caffeine contents, φ_{caf}, in the films were 0.1, 2.5, 5, 7, 10, 14.9 and 20 wt%, see Supplementary Material SM1 for details.

The light transmitted through the films with thickness ranging from 100 μm to 150 μm was measured at 600 nm (at this wavelength there is no light absorbance), in a Beckmann-Coulter DU650 spectrophotometer. The morphology of films was evaluated by SEM in a SEM-FEG JEOL JSM7401F microscope. The images were taken from the top side and from internal region (cryofracture) of the films. The surfaces were coated with a 2 nm thick gold layer prior to the analyses. Films were analyzed by Fourier transform infrared vibrational spectroscopy in the attenuated total reflectance mode in an Alpha FTIR-ATR, Bruker equipment, with a diamond crystal, accumulating 64 scans at 2 cm^{-1} of resolution. Differential scanning calorimetry (DSC) analyses were performed in a Q10 TA Instruments equipment, at 20 °C min^{-1} heating rate from 20 to 150 °C. The glass transition temperature (T_g) was determined from the second heating run. Thermogravimetric analyses (TGA) were performed with a Mettler Toledo TGA system, using temperature program from 30 °C to 950 °C at a heating rate of 5 °C/min under nitrogen atmosphere.

Density Functional Theory (DFT) calculations were performed using software Gaussian 09 [21] with the B3LYP functional and the 6-31 + G(d,p) as basis set.

2.4. In vitro release of caffeine from micrometric CAB/caf films

The release of caffeine from CAB/caf 2.5 wt%, 5 wt% and 7 wt% was investigated by immersing them (typically 10–15 mg film) in 7.0 mL of MilliQ water (pH 5.5), NaCl 0.010 mol L^{-1} (pH 5.5), NaCl 0.10 mol L^{-1} (pH 5.5), phosphate saline buffer (PBS, pH 7.4), HCl 0.010 mol L^{-1} (pH 2) or NaOH 1.0 × 10^{-5} mol L^{-1} (pH 9). An aliquot of 1.0 mL was withdrawn from the supernatant at pre-determined time intervals up to 48 h. After each sampling, the same volume of solvent was added to the medium to keep the solution volume constant. The release of caffeine to the medium was monitored by measuring the absorbance of withdrawn supernatants by UV spectrophotometry at 272 nm and (24 ± 1) °C. The calibration curve of caffeine taken at 272 nm was provided as Supplementary Material SM2.

3. Results and discussion

Caffeine is soluble in solvents with high dielectric constant. Upon drying, the caffeine molecules tend to crystalize. Fig. 2a and b shows SEM images of needle-shaped crystals of caffeine grown on Si/SiO_2 wafers by evaporation from acetone. Fig. 2c and d shows the optical microscopy and the corresponding CFM image of caffeine crystals on glass slides. The needle-shaped caffeine crystals were also observed after evaporation of nitromethane, dimethyl sulfoxide [22] and dichloromethane [23]. The crystallization process is driven by self-assembling of caffeine molecules through π-stacking interactions [24] and hollow tubular structures result from a diffusion limited crystal

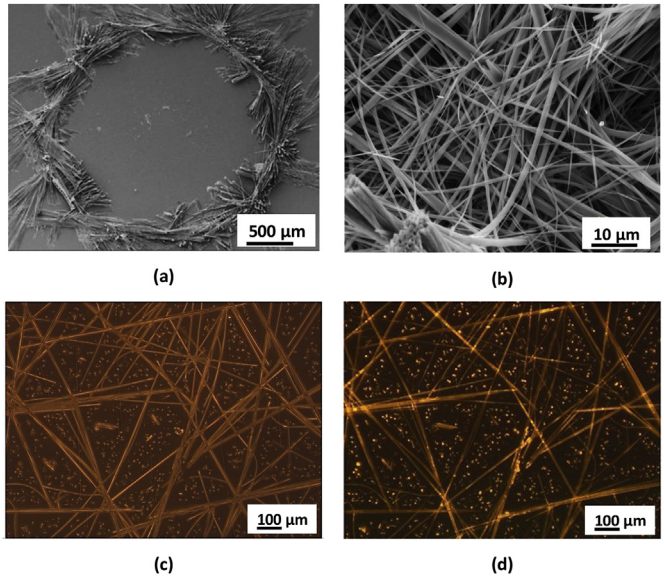

Fig. 2. (a) and (b) SEM images of needle-shaped crystals of caffeine grown on Si/SiO_2 wafers by evaporation from acetone.(c) Optical microscopy and the corresponding and (d) CFM image of caffeine crystals on glass slides, after acetone evaporation. The concentration of caffeine in acetone was 2.0 g L^{-1}.

growth [22]. In the CFM image (Fig. 2d) it is evident that part of caffeine molecules are arranged as long needles and part of them formed small aggregates.

3.1. CAB/caf spin-coated films

The effect of polymer concentration on the morphology of CAB5/caf, CAB10/caf, CAB20/caf spin-coated films is presented in the SEM images in Fig. 3a, b and 3c. The thickness of spin-coated films ranged from ~40 nm to ~80 nm, as determined by ellipsometry. The solvents used to prepare CAB and caffeine solutions were EA and acetone, respectively. Regardless of the CAB concentration, the caffeine needles appeared buried in the polymer or appeared as short needles scarcely distributed on the surface, as indicated by the arrows in Fig. 3a. The CFM images obtained for CAB5/caf films deposited on glass slides (Fig. 3d) corroborated with the SEM images; the caffeine structures

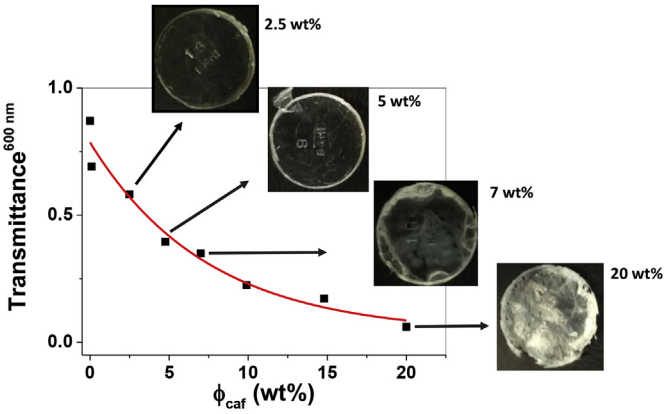

Fig. 4. Photographs and transmittance of light at 600 nm through the CAB/caf films as a function of caffeine content (ϕ_{caf}). The red line corresponds to the exponential fit $y = 0.75\ \exp(-x/7.4) + 0.036$, $R^2 = 0.9530$. The experimental data are mean values of duplicates, with standard deviations below 5%. (For interpretation of the references to colour in this figure legend, the reader is referred to the Web version of this article.)

appeared in the CFM image as short needles. These morphological features evidenced affinity between caffeine and CAB. For comparison, pure CAB spin-coated film showed no fluorescence, it appears completely dark in Fig. 3e. Pure CAB (Fig. 3f) and CAB20/caf (Fig. 3c) films presented "breath-figure" structures on the surface. "Breath figures" are cavities resulting from the condensation of the droplets of water on polymer solution during solvent evaporation and film formation [25,26].

3.2. CAB/caf cast films

Films of pure CAB are transparent. However, as the caffeine content (ϕ_{caf}) increased in the CAB/caf films, the transmittance of light through the films decreased exponentially and turned opaque, as shown in Fig. 4. Particularly, for ϕ_{caf} higher than 5 wt%, the turbidity presented by the films indicated phase separation between CAB and caffeine. Noteworthy, all films presented similar mean thickness values, which ranged from 100 µm to 150 µm. Fig. 5 shows SEM images taken from the top side and from the internal region (cryofracture) of pure CAB, CAB/caf 2.5 wt%, CAB/caf 5 wt% and CAB/caf 7 wt% films. Pure CAB

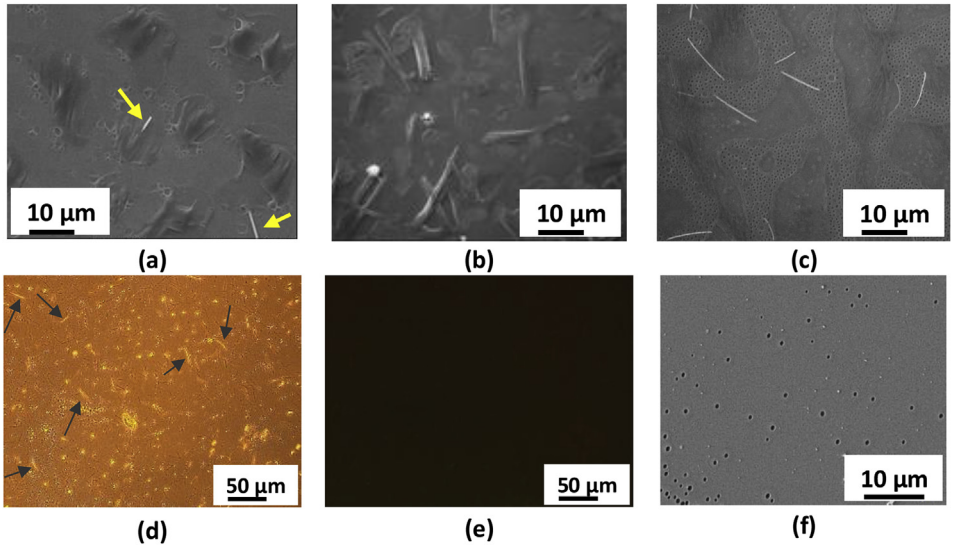

Fig. 3. SEM images of (a) CAB5/caf, (b) CAB10/caf, (c) CAB20/caf spin-coated films on Si/SiO_2 wafers. CFM images of (d) CAB5/caf films and (e) pure CAB films deposited from solution at 10 g L^{-1} in EA, on glass slides. (f) SEM image of pure CAB spin-coated film from solution at 10 g L^{-1} in EA, on Si/SiO_2 wafers.

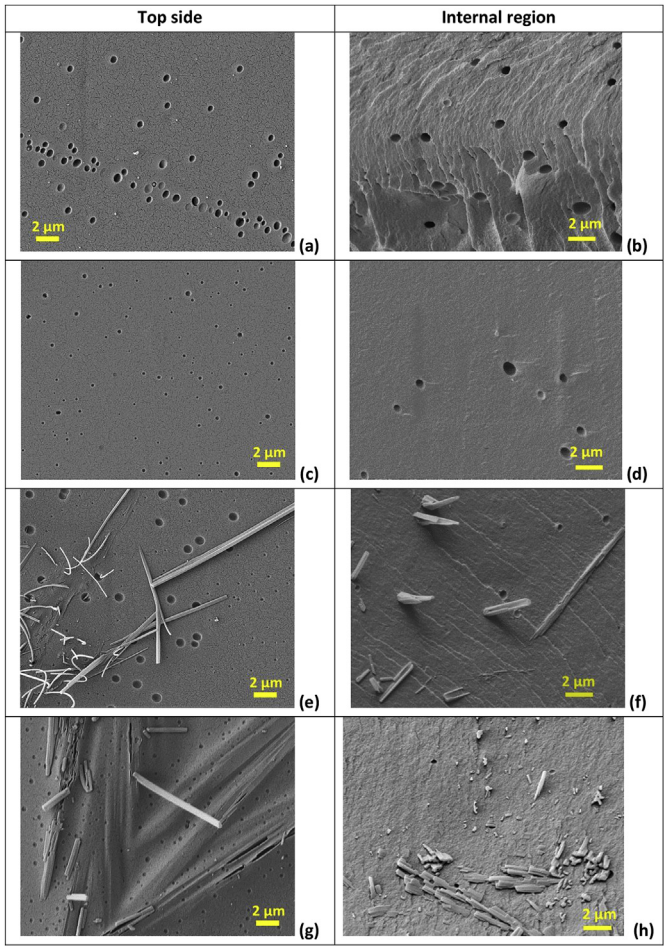

Fig. 5. SEM images of (a,b) pure CAB, (c,d) CAB/caf 2.5 wt%, (e,f) CAB/caf 5 wt% and (f,h) CAB/caf 7 wt% films.

Table 1
Glass transition temperature (T_g), initial decomposition temperature ($T_{5\%}$), degradation temperature (T_{deg}) and char residue at 500 °C determined for pure CAB and CAB/caf 2.5 wt%, CAB/caf 5 wt% and CAB/caf 7 wt% films.

Sample	T_g (°C)	$T_{5\%}$	T_{deg} (°C)	Char (%)
CAB	107 ± 1	315	368 ± 1	5.9
CAB/caf 2.5 wt%	96 ± 1	293	376 ± 2	6.1
CAB/caf 5 wt%	88 ± 1	238	210 ± 1 377 ± 1	7.5
CAB/caf 7 wt%	79 ± 1	244	251 ± 1 375 ± 2	6.7

films (Fig. 5a and b) presented the typical breath figures [25]. CAB/caf 2.5 wt% films (Fig. 5c and d) showed no caffeine crystals films and the breath figures were less frequent, indicating miscibility among CAB and caffeine and explaining the high transmittance (Fig. 4). However, CAB/caf 5 wt% (Fig. 5e and f) and CAB/caf 7 wt% (Fig. 5g and h) films presented caffeine crystals buried in the matrix and exposed to the air, indicating phase separation. The exposed caffeine crystals probably scattered the light more efficiently, explaining the transmittance decrease (Fig. 4).

The glass transition temperature (T_g) values determined for pure CAB and CAB/caf films as a function of caffeine content (ϕ_{caf}) are presented in Table 1. Caffeine itself has no T_g, but it presents melting point at 235 °C [27]. The T_g value determined for pure CAB (107 ± 1 °C) is in agreement with literature data [28]. The T_g values of CAB/caf films decreased linearly with ϕ_{caf}, so that the addition of each

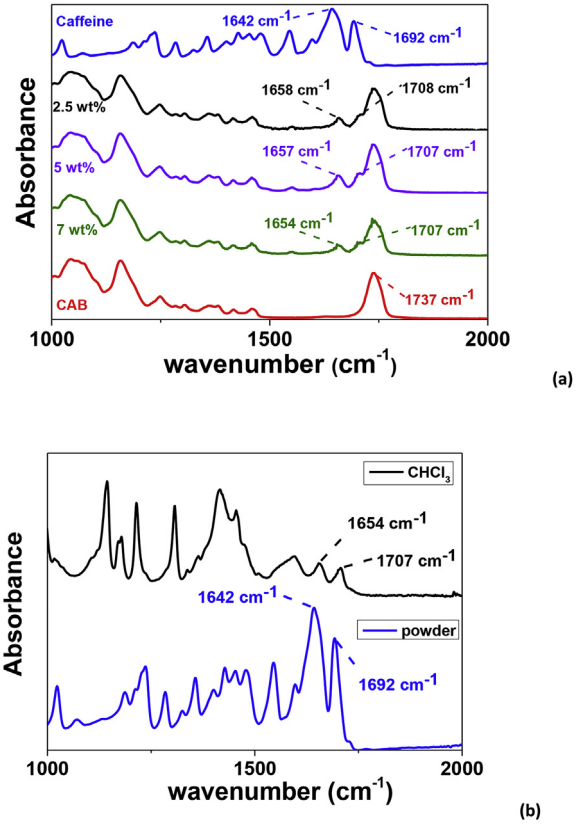

Fig. 6. FTIR-ATR determined for (a) pure caffeine as powder, pure CAB, CAB/caf 2.5 wt%, CAB/caf 5 wt% and CAB/caf 7 wt% films micrometric films, (b) pure caffeine as powder and caffeine dissolved in chloroform at 2.0 g L^{-1}.

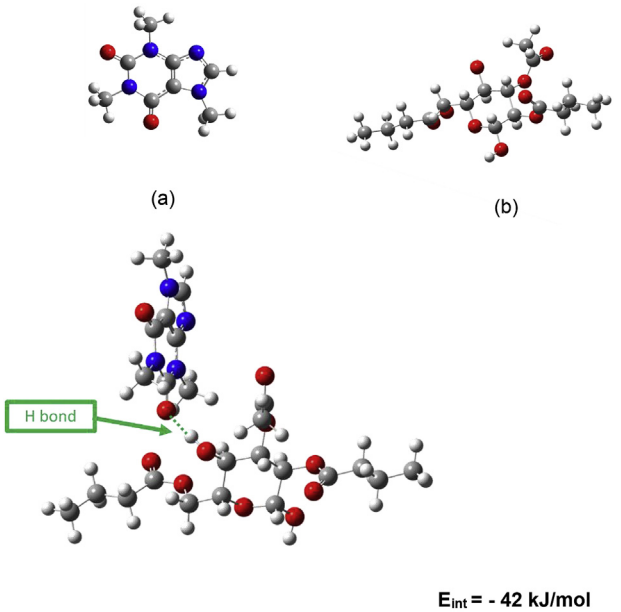

Fig. 7. Optimized geometries from DFT calculations of (a) caffeine, (b) CAB monomer and (c) caffeine and CAB interaction, where caffeine molecule approaches to CAB monomer by hydrogen bonding between CAB hydroxyl group and caffeine C=O(2). The interaction energy value was obtained from the difference of the energy of the isolated species.

1 wt% caffeine to CAB reduced its T_g in 3.8 °C, indicating favorable interactions between caffeine and CAB (Supplementary Material SM3). The T_g of alginate based microcapsules decreased from 74 °C to 71 °C

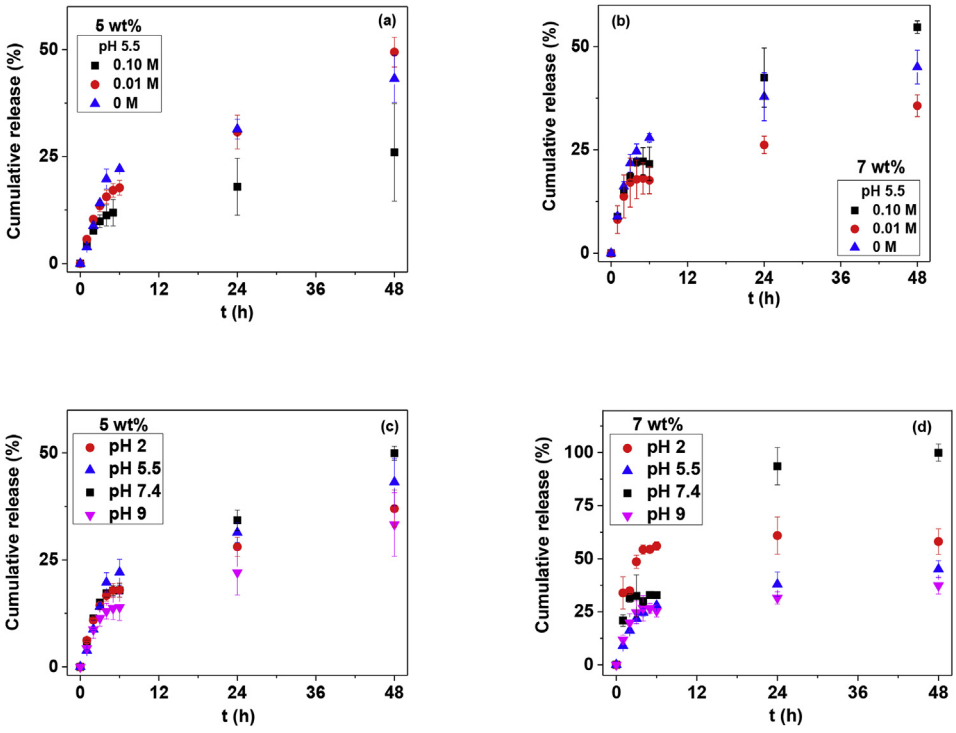

Fig. 8. Release profiles of caffeine from (a) CAB/caf 5 wt% and (b) CAB/caf 7 wt% in MilliQ at pH 5.5, 25 °C, in MilliQ water (blue triangle), NaCl 0.01 mol L^{-1} (red circle) and NaCl 0.10 mol L^{-1} (black square). Release profiles of caffeine from (c) CAB/caf 5 wt% and (d) CAB/caf 7 wt% at 25 °C, pH 2.0 (red circle), pH 5.5 (blue triangle), pH 7.4 (black square) and pH 9 (pink triangle). (For interpretation of the references to colour in this figure legend, the reader is referred to the Web version of this article.)

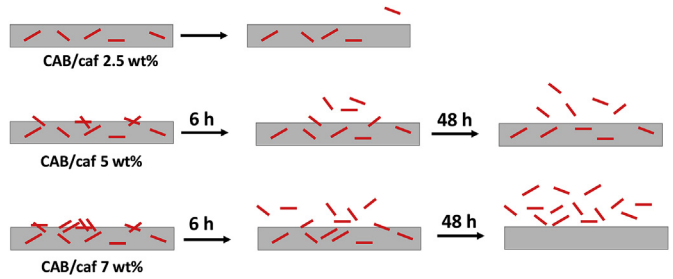

Fig. 9. Schematic representation of caffeine release pH 7.4, from CAB/caf 2.5 wt%, CAB/caf 5 wt% and CAB/caf 7 wt%, over the period of 6 h and 48 h.

due to the intermolecular hydrogen bonding with caffeine molecules [14]. Hydrogen bonds among caffeine molecules and poly(vinyl alcohol) also promoted the reduction of PVA T_g from 85 °C to 45 °C [27].

Supplementary Material SM4 provides the thermogravimetric curves and the corresponding derivative curves of CAB, CAB/caf 2.5 wt %, CAB/caf 5 wt% and CAB/caf 7 wt% films. Table 1 shows the temperatures corresponding to the initial decomposition temperature ($T_{5\%}$), thermal degradation (T_{deg}) and char residue values at 500 °C. The initial decomposition temperature ($T_{5\%}$) of pure CAB was noted at 315 °C and rest of the films exhibit ($T_{5\%}$) at 293 °C, 238 °C and 244 °C for CAB/caf 2.5 wt%, CAB/caf 5 wt% and CAB/caf 7 wt% respectively. The above results indicated that presence of caffeine content (ϕ_{caf}) decreases the thermal stability of CAB. The CAB/caf 2.5 wt% films presented only one thermal event, which was assigned to the main degradation, T_{deg}, at 376 °C; it is 8 °C higher than that of pure CAB and might be due to favorable interactions with caffeine. For CAB/caf 5 wt % and 7 wt% films, beyond the main decomposition at 377 °C and 375 °C, respectively, a small fraction of material underwent degradation at 210 °C and 251 °C, respectively, which might correspond to the segregated caffeine molecules that were observed on the film surface (Fig. 5e and g). The insignificant char residue obtained at 500 °C showed that CAB/caf systems undergo complete pyrolysis and decomposition.

The interactions between caffeine and CAB were further investigated using FTIR-ATR spectroscopy. Fig. 6a shows the FTIR-ATR spectra obtained for pure caffeine, pure CAB (powder), CAB/caf 2.5 wt %, CAB/caf 5 wt% and CAB/caf 7 wt% films, in the spectral range from 1000 cm^{-1} to 2000 cm^{-1}. Spectra with spectral range from 600 cm^{-1} to 4000 cm^{-1} and the corresponding bands assignments are provided as Supplementary Material SM5. The most interesting features concern the pure caffeine bands at 1642 cm^{-1} and 1692 cm^{-1}, assigned to the stretching of conjugated C=O(6) and isolated C=O(2) carbonyl groups [29]. In the presence of CAB, they shifted to higher wavenumber, for instance, CAB/caf 2.5 wt%, 5 wt% and 7 wt% films the C=O(6) bands shifted to 1658 cm^{-1}, 1657 cm^{-1}, and 1654 cm^{-1}, respectively, whereas the C=O(2) band shifted to 1707 cm^{-1}, in all compositions. The same effect was observed when the spectrum of caffeine powder was compared with the spectrum of caffeine dissolved in chloroform (Fig. 6b). In chloroform, where the caffeine molecules are well solvated, the C=O(6) and C=O(2) bands appeared at 1654 cm^{-1} and 1707 cm^{-1}. Thus, such shifts to higher wavenumber clearly indicate weakening of self-assembling of caffeine molecules and evidence favorable interactions between caffeine and CAB [30]. Considering the CAB DS_{Ac} of 0.2 and DS_{But} of 2.5, dipole-dipole interactions and van der Waals interactions are expected to drive the miscibility.

One should notice that during the FTIR-ATR analysis, the evanescent wave penetrates the whole CAB/caf film because the films thicknesses ranged from 30 μm to 50 μm thick, so that the spectra reveal the vibrational bands of functional groups present on the surface and in the bulk film. Recently, FTIR-ATR was applied as analytical tool to estimate the amount of caffeine and loperamide hydrochloride printed on poly (ethylene terephthalate) films [31].

DFT calculations were performed in order to gain insight about the interactions between caffeine and CAB monomer. The optimized DFT geometry of caffeine interacting with CAB monomer is displayed in Fig. 7. The geometry optimization steps indicated hydrogen bonding between CAB hydroxyl group and caffeine C=O(2), with interaction energy of - 42 kJ/mol. The geometry optimization steps are available as a movie at http://www.youtube.com/watch?v=FIXSQNvaFBw [32].

Table 2
Some examples of polymeric delivery systems for caffeine and the corresponding highlight and reference.

System	Highlight	Ref.
Alginate-based blends consisting of carrageenan, pectin, chitosan or psyllium husk powder	Chitosan coated beads released 50% of caffeine after 13 min.	[12]
Beta-glucan, resistant starch, and beta-cyclodextrin microparticles	Caffeine release was more prevalent in simulated intestinal juice than gastric medium, displaying controlled release mechanism for such systems.	[13]
Alginate-based matrix combined with different natural biopolymers	80% released in simulated mouth conditions after 30 min	[14]
Tablets with linseed polysaccharides	Buffers of pH 1.2, 6.8, 7.4, and DI water were used. Negligible drug release (< 10%) was noted at pH 1.2 (2 h). Higher and sustained release was observed at pH 6.8 and 7.4 up to 16 h	[16]
Microfibrillated celulose coated paper loaded with caffeine at 7 g/m^2	Release in 500 mL water, 100% caffeine release after10 h.	[19]
Acrylic acid (AAc), and 2-*N*,*N*-dimethylamino ethyl methacrylate grafted onto PVDF membrane.	At pH 5, the maximum release was reached at 3 h, while at pH 7, it took 5 h.	[34]
3D printed filaments of PVA/caffeine/paracetamol, with 4.7% and 9.5% caffeine	100% drug release in less than 360 min.	[27]
Chitosan–quercetin-poly(*N*-isopropylacrylamide) hydrogels, 0.85 mg/mL caffeine loaded	After 30 min, at 40 °C and pH 2.0, 50% drug release (burst effect). At pH 7 and 25 °C or 40 °C, sustained release.	[35]
Poly[*N*-isopropylacrylamide-*co*-(3-methacryloxypropyltrimethoxysilane)] (pNS) copolymer chains as the backbone and silica nanoparticles (SiP) as crosslinkers	Release in 150 mL deionized water (pH 6.8) or pH 1.7. The release reached equilibrium (93% release) within 4 h at both pH conditions.	[36]
Plasma treated polyamide 6,6 fibers impregnated with caffeine aqueous solution at 1%	Release in 150 mL PBS buffer at 37 °C. 90% release during the first hour.	[37]
Electrospun nanofibers of PVA/caffeine at weight ratio 25:1	Burst- caffeine released 100% within 60 s.	[38]
Bio cellulose membrane loaded with caffeine at 8 mg/cm^2	80% released in PBS after 5 min.	[39]
Magnetic alginate beads loaded with 100 mg caffeine	Diffusion of drug from hydrogels was controlled by the pH of environment; maximal release was 60% after ~3 h.	[40]
CAB/caf 7 wt%	Sustained release over 48 h. Total (1.5 g L^{-1}) released in PBS after 48 h.	This work

3.3. In vitro release of caffeine from CAB/caf films

The *in vitro* release of caffeine from CAB/caf 2.5 wt% films was negligible, regardless of the pH or ionic strength of external medium The miscibility between CAB and caffeine at ϕ_{caf} 2.5 wt% probably favored the homogeneous distribution of caffeine in the polymeric matrix, as evidenced in Fig. 5c and d, impairing the caffeine release to the medium.

Fig. 8a and b shows the cumulative release of caffeine from CAB/caf 5 wt% and 7 wt%, respectively, at pH 5.5, in MilliQ water, NaCl 0.01 mol L^{-1} and NaCl 0.10 mol L^{-1}. It is possible to divide the release behavior into two regimes, a fast one up to 6 h, and a slow and continuous one for longer release time (48 h). The fast process probably corresponds to the dissolution and release of caffeine located at the film surface (Fig. 5e and g), whereas the slow one refers to the release of caffeine buried in the films, as observed in SEM images (Fig. 5f and h). Small defects in the film structure (microcracks, for instance) are already enough to promote the release of caffeine from the bulk film. In a similar process, the release of caffeine from nanoporous network formed by MFC coated on paper also presented a fast release in the first 30 min, and a slow step until the total release took place, after 10 h [19]. At 6 h release, the amounts of caffeine released from CAB/caf 5 wt % and CAB/caf 7 wt% in MilliQ water were the most pronounced, 22.1 ± 0.5% and 28 ± 1%, respectively. After 48 h, the highest cumulative releases amounted to 43 ± 6% from CAB/caf 5 wt% in MilliQ water and 55 ± 2% from CAB/caf 7 wt% in NaCl 0.10 mol L^{-1}.

The fast (up to 6 h) and slow release stages were also observed for the release under different pH values (Fig. 8c and d). In the fast stage, the release from CAB/caf 5 wt% showed weak pH dependence; it ranged from 14 ± 3% at pH 9 to 22 ± 3% at pH 5.5. On the other hand, the release from CAB/caf 7 wt% was the highest at pH 2 (56 ± 2%) and the lowest at pH 9 (25 ± 3%). After 48 h, at pH 7.4, the release of caffeine from CAB/caf 7 wt% and CAB/caf 5 wt% films was 98 ± 2% and 50 ± 2%, respectively, which correspond to 1.5 g L^{-1} and 0.5 g L^{-1} caffeine.

Fig. 9 shows schematically the release of caffeine at pH 7.4, from CAB/caf 2.5 wt%, CAB/caf 5 wt% and CAB/caf 7 wt%, over the period of 6 h and 48 h. In this model, caffeine molecules are not released from CAB/caf 2.5 wt% films due to complete miscibility with CAB, which does not swell in this medium. In the case of CAB/caf 5 wt% and CAB/caf 7 wt%, in the first 6 h, caffeine molecules located on the film surface dissolve in the medium. This first step is slow because caffeine molecules, which are not miscible with CAB, are well packed into organized structures on the outer surface, as observed in Fig. 5e and g. This process depends mainly on the amount of caffeine that segregated from the CAB matrix. After dissolution of external caffeine molecules, caffeine molecules located in the interior of the CAB films can take advantage of breath figures or film degradation to come in contact with the external medium, and then, to diffuse to the medium. Supplementary Material SM6 shows photographs of CAB/caf 2.5 wt% films and CAB/caf 7 wt% films and after 48 h, at pH 7.4. CAB/caf 2.5 wt % films kept their homogeneous and regular appearance, indicating that CAB was not eroded by the medium. On the other hand, CAB/caf 7 wt% films show empty (dark) spots, which probably were previously occupied by caffeine molecules.

Many empirical models for drug release are designed for erodible polymers [33], which is not the case of CAB under the experimental conditions. CAB is chemically stable in the pH range investigated (pH 2 to pH 9). Supplementary Material SM7 provides an attempt to fit the experimental data to the Korsmeyer-Peppas model:

$$\frac{M^t}{M^{eq}} = kt^n \quad (1)$$

where M^t is the released amount at time "t", M^{eq} is the released amount at equilibrium, k is a constant and "n" is the diffusional coefficient, which is related to the interaction between drug and polymer matrix and describes the release mechanism. The fittings were performed for the first 6 h, where only the dissolution of segregated caffeine molecules takes place. The resulting "n" values ranged from 0.67 to 1.0 (Supplementary Material SM7), indicating weak interaction between polymer and drug. This is consistent with the proposed model, which considers the first step as the dissolution period of segregated caffeine molecules. For period longer than 6 h, the release rate was estimated from linear fits (between 6 h and 48 h) in the range of 5 mg L^{-1} h^{-1} to 8 mg L^{-1} h^{-1}.

Table 2 shows some literature examples [12–14,16,19,26,34–40], which employed polymer matrices for the release of caffeine. Many of them are water soluble polymers or polymers that swell in aqueous

media. However, in comparison to CAB/caf 7 wt%, most of them presented faster release of caffeine, pointing out that for hydrophilic drugs, as caffeine, water soluble polymers provide pronounced contact with water, speeding up the release.

4. Conclusions

The comprehension about the miscibility of drug and the polymer carrier is important to understand the release process over a specific duration. In this study, partial miscibility of CAB and caffeine was observed for caffeine contents higher than 5 wt%; total miscibility was observed for caffeine content lower than 2.5 wt%. The release from completely miscible systems was impaired. Systems partially miscible showed a two-step release process, namely, a first one corresponding to the dissolution of segregated drug and a second one related to the dissolution and release of drug located in the internal polymer matrix. CAB/caf 7 wt% films were particularly interesting because they provided total release of loaded caffeine at pH 7.4, for the prolonged period of 48 h. This feature is particularly advantageous for systems, which require prolonged release of caffeine. Moreover, CAB/caf 7 wt% systems might be interesting for hot melt extrusion because both components can be processed together and the caffeine content of 7 wt% is similar to those found in commercial tablets for headache as 6.5 wt% [41].

CRediT authorship contribution statement

Laíse M. Furtado: Conceptualization, Methodology, Investigation. **Karina C.P. Hilamatu:** Methodology, Investigation. **Krishnasamy Balaji:** Formal analysis. **Rômulo A. Ando:** Writing - review & editing, Software, Supervision. **Denise F.S. Petri:** Writing - review & editing, Funding acquisition, Supervision, Project administration.

Declaration of competing interest

The authors declare that they have no known competing financial interests or personal relationships that could have appeared to influence the work reported in this paper.

Acknowledgements

Authors gratefully acknowledge financial support from Brazilian Funding Agency “Conselho Nacional de Desenvolvimento Científico e Tecnológico” (CNPq Grants 161116/2018-3, 171250/2017, 306848/2017, 421014/2018).

Appendix A. Supplementary data

Supplementary data to this article can be found online at https://doi.org/10.1016/j.jddst.2019.101472.

References

[1] K.J. Edgar, C.M. Buchanan, J.S. Debenham, P.A. Rundquist, B.D. Seiler, M.C. Shelton, D. Tindall, Advances in celulose ester performance and application, Prog. Polym. Sci. 26 (2001) 1605–1688.
[2] K.J. Edgar, Cellulose esters in drug delivery, Cellulose 14 (2007) 49–64.
[3] J. Varshosaz, S. Taymouri, E. Jafari, A. Jahanian-Najafabadi, A. Taheri, Formulation and characterization of cellulose acetate butyrate nanoparticles loaded with nevirapine for HIV treatment, J. Drug Deliv. Sci. Technol. 48 (2018) 9–20.
[4] M.C.C.M. Sobral, A.J.F.N. Sobral, J.T. Guthrie, M.H. Gil, Ketotifen controlled release from cellulose acetate propionate and cellulose acetate butyrate membranes, J. Mater. Sci. Mater. Med. 19 (2008) 677–682.
[5] J. Shokri, K. Adibkia, Application of cellulose and cellulose derivatives, in: T. van de Ven, L. Godbout (Eds.), Pharmaceutical Industries. Cellulose - Medical, Pharmaceutical and Electronic Applications, IntechOpen, 2013, https://doi.org/10.5772/55178.
[6] R. Ali, M. Walther, R. Bodmeier, Cellulose acetate butyrate: Ammonio methacrylate copolymer blends as a novel coating in osmotic tablets, AAPS PharmSciTech 19 (2017) 148–154.
[7] P.M. Kosaka, Y. Kawano, O.A. El Seoud, D.F.S. Petri, Catalytic activity of lipase immobilized onto ultrathin films of cellulose esters, Langmuir 23 (2007) 12167–12173.
[8] J. Amim Jr., D.F.S. Petri, Effect of amino-terminated substrates onto surface properties of cellulose esters and their interaction with lectins, Mater. Sci. Eng. C 32 (2012) 348–355.
[9] T. Al Reef, E. Ghanem, Caffeine: well-known as psychotropic substance, but little as immunomodulatory, Immunobiology 223 (2018) 818–825.
[10] J. Blanchard, S.J.A. Sawers, The absolute bioavailability of caffeine in man, Eur. J. Clin. Pharmacol. 24 (1983) 93–98.
[11] H.C. Yew, M. Misran, Preparation and characterization of pH dependent κ-carrageenan-chitosan nanoparticle as potential slow release delivery carrier, Iran. Polym. J. 25 (2016) 1037–1046.
[12] A. Belščak-Cvitanović, D. Komes, S. Karlović, S. Djaković, I. Špoljarić, G. Mršić, D. Ježek, Improving the controlled delivery formulations of caffeine in alginate hydrogel beads combined with pectin, carrageenan, chitosan and psyllium, Food Chem. 167 (2015) 378–386.
[13] N. Noor, A. Shah, A. Gani, A. Gani, F.A. Masoodi, Microencapsulation of caffeine loaded in polysaccharide based delivery systems, Food Hydrocolloids 82 (2018) 312–321.
[14] N. Mohammadi, M.R. Ehsani, H. Bakhoda, Development of caffeine-encapsulated alginate-based matrix combined with different natural biopolymers, and evaluation of release in simulated mouth conditions, Flavour Fragrance J. 33 (2018) 357–366.
[15] A.M. Nikoo, R. Kadkhodaee, B. Ghorani, H. Razzaq, N. Tucker, Electrospray-assisted encapsulation of caffeine in alginate micro hydrogels, Int. J. Biol. Macromol. 116 (2018) 208–216.
[16] M.T. Haseeb, M.A. Hussain, S. Bashir, M.U. Ashraf, N. Ahmad, Evaluation of superabsorbent linseed-polysaccharides as a novel stimuli-responsive oral sustained release drug delivery system, Drug Dev. Ind. Pharm. 43 (2017) 409–420.
[17] N. Harada, J.I. Nakamura, H. Uyama, Preparation of macroporous cellulose beads through a single-step non-solvent induced phase separation method from a cellulose acetate solution, Bull. Chem. Soc. Jpn. 92 (2019) 1444–1446.
[18] Y. Yang, W. Li, D.G. Yu, G. Wang, G.R. Williams, Z. Zhang, Tunable drug release from nanofibers coated with blank cellulose acetate layers fabricated using tri-axial electrospinning, Carbohydr. Polym. 203 (2019) 228–237.
[19] N. Lavoine, I. Desloges, J. Bras, Microfibrillated cellulose coatings as new release systems for active packaging, Carbohydr. Polym. 103 (2014) 528–537.
[20] V. Malaterre, J. Ogorka, N. Loggia, R. Gurny, Oral osmotically driven systems: 30 years of development and clinical use, Eur. J. Pharm. Biopharm. 73 (2009) 311–323.
[21] Gaussian 09, Revision A.02, M.J. Frisch, G.W. Trucks, H.B. Schlegel, G.E. Scuseria, M.A. Robb, J.R. Cheeseman, G. Scalmani, V. Barone, G.A. Petersson, H. Nakatsuji, X. Li, M. Caricato, A. Marenich, J. Bloino, B.G. Janesko, R. Gomperts, B. Mennucci, H.P. Hratchian, J.V. Ortiz, A.F. Izmaylov, J.L. Sonnenberg, D. Williams-Young, F. Ding, F. Lipparini, F. Egidi, J. Goings, B. Peng, A. Petrone, T. Henderson, D. Ranasinghe, V.G. Zakrzewski, J. Gao, N. Rega, G. Zheng, W. Liang, M. Hada, M. Ehara, K. Toyota, R. Fukuda, J. Hasegawa, M. Ishida, T. Nakajima, Y. Honda, O. Kitao, H. Nakai, T. Vreven, K. Throssell, J.A. Montgomery Jr., J.E. Peralta, F. Ogliaro, M. Bearpark, J.J. Heyd, E. Brothers, K.N. Kudin, V.N. Staroverov, T. Keith, R. Kobayashi, J. Normand, K. Raghavachari, A. Rendell, J.C. Burant, S.S. Iyengar, J. Tomasi, M. Cossi, J.M. Millam, M. Klene, C. Adamo, R. Cammi, J.W. Ochterski, R.L. Martin, K. Morokuma, O. Farkas, J.B. Foresman, D.J. Fox, Gaussian, (2016) Wallingford CT.
[22] M.D. Eddleston, W. Jones, Formation of tubular crystals of pharmaceutical compounds, Cryst. Growth Des. 10 (2010) 365–370.
[23] A. Sarfraz, A. Simo, R. Fenger, W. Christen, K. Rademann, U. Panne, F. Emmerling, Morphological diversity of caffeine on surfaces: needles and hexagons, Cryst. Growth Des. 12 (2012) 583–588.
[24] L. Tavagnacco, S. Di Fonzo, F. D'Amico, C. Masciovecchio, J. Brady, A. Cesàro, Stacking of purines in water: the role of dipolar interactions in caffeine, Phys. Chem. Chem. Phys. 18 (2016) 13478–13486.
[25] L.S. Blachechen, M.A. Souza, D.F.S. Petri, Effect of humidity and solvent vapor phase on cellulose esters films, Cellulose 19 (2012) 443–457.
[26] G. Widawski, M. Rawiso, B. François, Self-organized honeycomb morphology of star-polymer polystyrene films, Nature 369 (1994) 387–389.
[27] A. Goyanes, J. Wang, A. Buanz, R. Martínez-Pacheco, R. Telford, S. Gaisford, A.W. Basit, 3D printing of medicines: engineering novel oral devices with unique design and drug release characteristics, Mol. Pharm. 12 (2015) 4077–4084.
[28] J. Amim Jr., L.S. Blachechen, D.F.S. Petri, Effect of sorbitan based surfactants on glass transition temperature of cellulose esters, J. Therm. Anal. Calorim. 107 (2012) 1259–1265.
[29] N.O. Johnson, T.P. Light, G. MacDonald, Y. Zhang, Anion-caffeine interactions studied by 13C and 1H NMR and ATR-FTIR spectroscopy, J. Phys. Chem. B 121 (2017) 1649–1659.
[30] P.J. Marsac, T. Li, L.S. Taylor, Estimation of drug–polymer miscibility and solubility in Amorphous solid dispersions using experimentally determined interaction parameters, Pharm. Res. 26 (2008) 139–151.
[31] M. Palo, K. Kogermann, N. Genina, D. Fors, J. Peltonen, J. Heinämäki, N. Sandler, Quantification of caffeine and loperamide in printed formulations by infrared spectroscopy, J. Drug Deliv. Sci. Technol. 34 (2016) 60–70.
[32] https://www.youtube.com/watch?v=IqaPsFcEaPc&feature=youtu.be.
[33] C. Mircioiu, V. Voicu, V. Anuta, A. Tudose, C. Celia, D. Paolino, M. Fresta, R. Sandulovici, I. Mircioiu, Mathematical modeling of release kinetics from supramolecular drug delivery systems, Pharmaceutics 11 (2019) 140.
[34] G.M. Estrada-Villegas, G. González-Pérez, E. Bucio, Adsorption and release of

caffeine from smart PVDF polyampholyte membrane, Iran. Polym. J. 28 (2019) 639–647.
[35] G. Cirillo, M. Curcio, U.G. Spizzirri, O. Vittorio, E. Valli, A. Farfalla, A.L. Fiore, P. Nicoletta, F. Iemma, Chitosan–quercetin bioconjugate as multi-functional component of Antioxidants and dual-responsive hydrogel networks, Macromol. Mater. Eng. 304 (2019) 1800728.
[36] M.A. Alam, M. Takafuji, H. Ihara, Silica nanoparticle-crosslinked thermosensitive hybrid hydrogels as potential drug-release carriers, Polym. J. 46 (2014) 293–300.
[37] C. Labay, J.M. Canal, C. Canal, Relevance of surface modification of polyamide 6.6 fibers by air plasma treatment on the release of caffeine, Plasma Process. Polym. 9 (2012) 165–173.
[38] X. Li, M.A. Kanjwal, L. Lin, I.S. Chronakis, Electrospun polyvinyl-alcohol nanofibers as oral fast-dissolving delivery system of caffeine and riboflavin, Colloids Surf., B 103 (2013) 182–188.
[39] N.H.C.S. Silva, I. Drumond, I.F. Almeida, P. Costa, C.F. Rosado, C. Pascoal Neto, C.R.S. Freire, A.J.D. Silvestre, Topical caffeine delivery using biocellulose membranes: a potential innovative system for cellulite treatment, Cellulose 21 (2014) 665–674.
[40] M. Amiri, M. Salavati-Niasari, A. Pardakhty, M. Ahmadi, A. Akbari, Caffeine: a novel green precursor for synthesis of magnetic CoFe2O4 nanoparticles and pH-sensitive magnetic alginate beads for drug delivery, Mater. Sci. Eng. C 76 (2017) 1085–1093.
[41] https://www.drugs.com/dosage/acetaminophen-caffeine.html , Accessed date: September 2019.